Crystal Structure of the Clathrate Form of Syndiotactic Poly(p-methylstyrene) Containing o-Dichlorobenzene

Vittorio Petraccone,[†] Domenico La Camera,*,[†] Lucia Caporaso,[‡] and Claudio De Rosa[†],*

Dipartimento di Chimica, Università di Napoli "Federico II", Via Mezzocannone 4, 80134 Napoli, Italy; and Dipartimento di Chimica, Università di Salerno, I-84081 Baronissi (SA), Italy

Received November 16, 1999; Revised Manuscript Received January 18, 2000

ABSTRACT: The crystal structure of the clathrate form of syndiotactic poly(p-methylstyrene) (s-PPMS) containing o-dichlorobenzene (o-DCB) is presented. The structure is characterized by polymer chains in **s**(2/1)2 helical conformation and o-dichlorobenzene molecules packed in a monoclinic unit cell with axes $a = 23.4$ Å, $b = 11.8$ Å, $c = 7.7$ Å, and $\gamma = 115°$, according to the space group $P2_1/a$. The calculated crystalline density is 1.07 g/cm^3 for two polymer chains (eight monomer units) and two o-DCB molecules included in the unit cell. The o-DCB molecules occupy cavities delimited by the phenyl rings of two enantiomorphic polymer chains. A disorder in the positioning of the o-DCB molecules inside the cavity is present. A comparison with the crystal structure of the clathrate form of s-PPMS containing tetrahydrofuran is presented. Remarkable differences were found, confirming the previous hypothesis that two different types of crystal structures (α and β class) are presented by the clathrate forms of s-PPMS depending on the guest molecule.

Introduction

Syndiotactic poly(p-methylstyrene) (s-PPMS) presents a complex polymorphic behavior: four different crystalline forms (named forms I, II, III and V), one mesomorphic form (form IV) and several clathrate forms, containing in the crystalline phase molecules of a second chemical species, have been found so far.[1,2] X-ray fiber diffraction data[2] of the various forms, as well as solid state ^{13}C NMR[3] and FTIR[4] studies, have shown that in forms I and II and in all the clathrate forms, the s-PPMS chains adopt a **s**(2/1)2 helical conformation (TTGG)$_2$, with a repetition period of 7.7 Å, whereas forms III, IV, and V are characterized by chains in *trans*-planar conformation, with a repetition period of 5.1 Å.

The interesting property of s-PPMS to form clathrate structures containing low molecular weight substances trapped in the cavities of the crystalline lattice, have been also found for syndiotactic polystyrene (s-PS).[5−10] The interest for these structures rests with the possibility of using these forms in applications like, for instance, chemical separations and water and air purification from organic molecules.[11−13]

The clathrate forms of s-PPMS have been divided in two different classes, α and β.[14] This classification was based on either the analogies between X-ray powder diffraction patterns, or the different behavior with respect to suitable treatments involving the removal of guest molecules (e.g., annealing and acetone treatments).[14] The α class includes clathrates of s-PPMS containing o-dichlorobenzene (o-DCB), o-xylene, o-chlorophenol, and N-methyl-2-pyrrolidone, which have similar X-ray powder diffraction patterns, and transform into form I of s-PPMS upon annealing or acetone treatments.[14] The β class includes the clathrate forms of s-PPMS containing tetrahydrofuran (THF), benzene, cyclohexane, cyclohexanone, and 1,4-dioxane, whose X-ray powder diffraction patterns are very similar,

but differ from those of the clathrate of the α class. The β class clathrates are transformed into form II by annealing or acetone treatments.[14]

Only the crystal structure of the clathrate form of s-PPMS including THF, representative of the β class, has been solved so far;[15] chains in **s**(2/1)2 helical conformations and four THF molecules are packed in a monoclinic unit cell, with axes $a = 18.8$ Å, $b = 12.7$ Å, $c = 7.7$ Å, and $\gamma = 100°$, according to the space group $P2_1/a$. A preliminary model of the clathrate form of s-PPMS with o-DCB, based on electron diffraction data, has been suggested in a previous paper.[16] In the present paper a detailed model of the crystal structure of the clathrate form of s-PPMS including o-DCB, determined by X-ray diffraction and packing energy calculations, is presented. This structure is representative of the α class clathrates of s-PPMS.

Experimental Part and Method of Calculation

The s-PPMS was synthesized in our laboratories with homogeneous catalytic system based on tetrabenzyltitanium and methylalumoxane, according to the procedure described in ref 1. The polymer fraction insoluble in 2-butanone was used. The syndiotacticity of the polymer was evaluated by ^{13}C NMR; the fraction of *rrrr* pentads was higher than 95%.

Unoriented samples of the clathrate form of s-PPMS containing o-DCB were obtained by casting, at room temperature, from 10 wt % o-DCB solution. Oriented fibers of the clathrate form were obtained by exposing fiber samples in the mesomorphic form IV to o-DCB vapor for 24 h at 35−45 °C, under the condition of fixed length.[2] Fibers of the mesomorphic form IV were obtained by stretching films of s-PPMS in form I at 130 °C.[1,2] Films of s-PPMS in form I were obtained by casting procedures from 10 wt % toluene solution, at 50 °C. The drawing of s-PPMS films was conducted with a Minimat apparatus with a strain rate of 2−3 mm/min.

Wide-angle X-ray diffraction patterns were obtained with nickel-filtered Cu Kα radiation. The diffraction patterns of oriented samples were obtained with a photographic cylindrical camera, whereas those for unoriented samples were recorded with an automatic Philips diffractometer.

The thermogravimetric analyses were carried out from room temperature to 200 °C with a Mettler TG50 Thermobalance

---

[†] Università di Napoli "Federico II".
[‡] Università di Salerno.
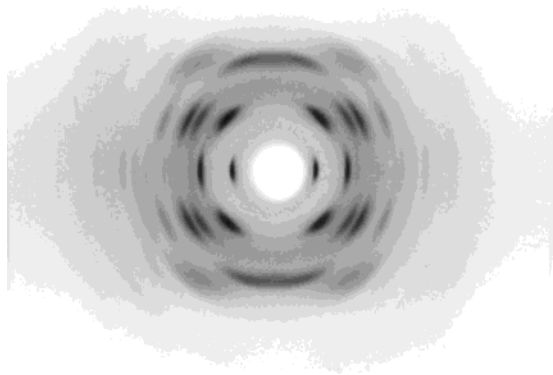
Figure 1. X-ray fiber diffraction pattern of the clathrate form of s-PPMS containing *o*-DCB.

in a flowing-nitrogen atmosphere at a heating rate of 10 K/min. In this range of temperature, no decomposition of the polymer occurs.

Calculated structure factors were obtained as $Fc = \sum|F_i|^2 M_i$, where M_i is the multiplicity factor and the summation is taken over all reflections included in the 2θ range of the corresponding spot observed in the X-ray fiber diffraction pattern. A thermal factor $B = 8$ Å² and atomic scattering factors from ref 17 were used. The observed structure factors F_o were evaluated from the intensities of the reflections observed in the X-ray fiber diffraction pattern, $F_o = (I_o/Lp)^2$, where Lp is the Lorentz–polarization factor for X-ray fiber diffraction: $Lp = (1 + \cos^2 2\theta)/[2(\sin^2 2\theta - \zeta^2)^{1/2}]$, with $\zeta = \lambda(l/c)$, l and c being the order of the layer line and the chain axis, respectively. The experimental intensities I_o were evaluated by the multiple film method and measured visually with an intensity scale. Owing to the different shape of the reflections on the equator and on the first layer and second layer, due to the different dimensions of the lamellar crystals in the directions normal and parallel to the chain axis, different factors have been used to scale observed and calculated structure factors on the different layer lines. The agreement R factor has been calculated as $R = \sum|F_o - F_c|/\sum F_o$.

The packing energy of the only s-PPMS chains (that is without the guest molecules) was evaluated as half the sum of the interaction energies between the atoms of one monomeric unit and all the surrounding atoms of the neighboring macromolecules. The packing energy of the guest *o*-DCB in the cavity was calculated as half the sum of the interaction energies between the atoms of the *o*-DCB molecule and all the atoms of the neighboring s-PPMS chains which delimit the cavity. The minimization of the energy was performed by using the program TINKER.[18] The interaction energies were calculated by using the 12–6 Lennard–Jones potential function, $E(r) = A(r^{-12}) - B(r^{-6})$, up to distances r equal to twice the sum of the van der Waals radii for each pair of atoms. The parameters for the nonbonded interactions reported by Flory,[19] taking the methyl group as a single rigid unit, were used.[20] The parameters involving the chlorine atoms have been derived according to the procedure of Suter and Flory[21] and Brant et al.[22] from the basic data of Ketelaar[23] (polarizability and van der Waals radius) and Hopfinger[24] (effective number of electrons). The conformation of the polymer chains and, hence the c axis, was kept constant in the calculations.

Results and Discussion

The X-ray fiber diffraction pattern of the clathrate form of s-PPMS with *o*-DCB is reported in Figure 1. All the reflections observed in the fiber pattern are listed in Table 1. The reflections are accounted for by a monoclinic unit cell with constants $a = 23.4$ Å, $b = 11.8$ Å, $c = 7.7$ Å, and $\gamma = 115°$, in agreement also with the electron diffraction data reported in a previous paper.[16]

Table 1. Diffraction Angles 2θ, Bragg Distances d, and Reciprocal Coordinates ξ and ζ of the Reflections Observed on the Layer Lines l of the X-ray Fiber Diffraction Pattern of the Clathrate Form of s-PPMS Containing o-Dichlorobenzene (Figure 1)

2θ (deg)	d (Å)	ξ (Å⁻¹)	ζ (Å⁻¹)	l
8.3	10.65	0.094	0	0
9.2	9.60	0.104	0	0
16.2	5.47	0.183	0	0
18.2	4.87	0.205	0	0
23.0	3.87	0.259	0	0
24.5	3.63	0.275	0	0
28.2	3.16	0.317	0	0
30.5	2.93	0.341	0	0
33.6	2.67	0.375	0.	0
12.2	7.28	0.044	0.130	1
14.1	6.12	0.988	0.130	1
15.6	5.69	0.118	0.130	1
16.8	5.28	0.138	0.130	1
20.1	4.43	0.185	0.130	1
21.9	4.05	0.210	0.130	1
23.2	3.83	0.226	0.130	1
26.6	3.35	0.268	0.130	1
30.1	2.97	0.310	0.130	1
24.4	3.64	0.089	0.260	2
26.4	3.38	0.141	0.260	2
28.1	3.16	0.178	0.260	2
29.8	2.99	0.209	0.260	2
33.0	2.71	0.261	0.260	2
38.8	2.32	0.344	0.260	2
40.8	2.21	0.370	0.260	2
43.0	2.10	0.397	0.260	2
45.8	1.98	0.433	0.260	2

The space group is $P2_1/a$, in agreement with the systematic absences of $hk0$ reflections with $h = 2n + 1$.

Thermogravimetric measurements on as-prepared powder samples, showing a X-ray crystallinity index of about 50–60% and a density, measured by flotation, of 1.1 g/cm³, indicate weight losses of about 25%. On the basis of these experimental data, a molar ratio monomer/ *o*-DCB in the crystal close to 4 was assumed. The crystalline density is 1.07 g/cm³, assuming two polymer chains in the **s**(2/1)2 helical conformation and two *o*-DCB molecules included in the unit cell.

To find possible packing models of s-PPMS chains, showing cavities that are able to accommodate *o*-DCB molecules, calculations of the packing energy of the only s-PPMS chains, without the guest molecules, were performed. The value of the conformational parameters of the **s**(2/1)2 helical chains of s-PPMS were assumed the same as that we found in the crystal structure of the clathrate form of s-PPMS with tetrahydrofuran.[15] The s-PPMS chains were positioned in the unit cell with their 2-fold screw axes coincident with the crystallographic 2-fold screw axes in the space group $P2_1/a$ (Figure 2). Packing energy calculations were performed keeping the parameters of the unit cell constant at the experimental values and varying the orientation (ω) and the height (z) of the chains. The angle of rotation ω of the chain around its axis and the height z are defined in Figure 2.

A map of the packing energy for the space group $P2_1/a$ is reported as a function of ω and z/c in Figure 3. The map is periodic over $\omega = 180°$ and $z/c = 0.5$; therefore, only the portion in the range $\omega = 0–180°$ and $z/c = 0.5–1.0$ is shown. The map presents an absolute minimum at $\omega = 15°$ and $z/c = 0.79$ Å and another minimum of higher energy. The analysis of the empty spaces in the packing models corresponding to the energy minima of Figure 3 has shown that only for the absolute energy minimum model (shown in Figure 2) there is plenty of
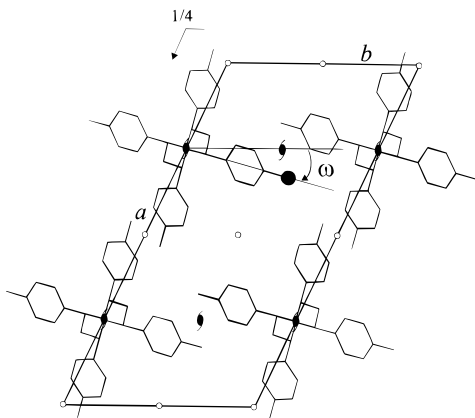
Figure 2. Definitions of the variables used in the packing energy calculations of the only s-PPMS chains. ω is the rotation angle of the **s**(2/1)2 helical chain of s-PPMS around the chain axis; it is positive for a clockwise rotation. The height of the carbon atom indicated by a filled circle defines the z coordinate. The crystallographic symmetry elements of the space group $P2_1/a$ are also shown. The orientation of the chains of s-PPMS in the unit cell corresponds to the absolute packing energy minimum ($\omega = 15°$) of the map of Figure 3.
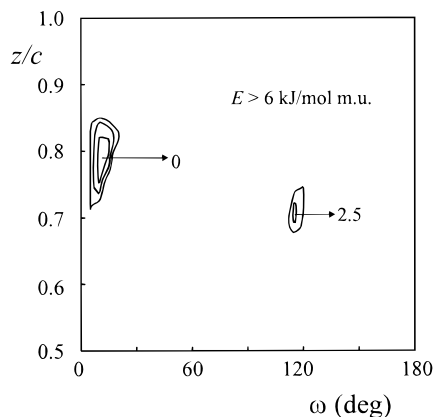
Figure 3. Map of the packing energy of the only s-PPMS chains as a function of ω and z/c for the space group $P2_1/a$. The curves are drawn at intervals of 2 kJ/mol of monomeric unit with respect to the absolute minimum of the map assumed as zero.

space for the inclusion of the *o*-DCB guest molecules. In this model there are empty spaces around the centers of symmetry of the lattice, located at $x/a = 0.5$, $y/b = 0.5$, $z/c = 0.5$; $x/a = 0$, $y/b = 0.5$, $z/c = 0$; and $x/a = 1.0$, $y/b = 0.5$, $z/c = 0$. Each cavity is delimited by two enantiomorphous chains (for instance, the cavity around the center of symmetry located at $x/a = 0.5$, $y/b = 0.5$, $z/c = 0.5$ is delimited by the two enantiomorphous chains with chain axes at $x/a = 0.25$, $y/b = 0$ and $x/a = 0.75$, $y/b = 1$) and is able to accommodate only one *o*-DCB molecule. This is in agreement with the previous considerations about the crystalline density and the thermogravimetric measurements.

The best position of the *o*-DCB molecules inside the unit cell was found by calculations of the packing energy of the guest *o*-DCB molecule inside the cavity. The calculations were performed by keeping the orientation of the s-PPMS chains constant, as in the position of the absolute minimum of Figure 3, and the energy was minimized by varying the position of the *o*-DCB molecule inside the cavity. As a starting point in the minimization procedure, the center of the phenyl ring of the *o*-DCB molecule was assumed to be coincident
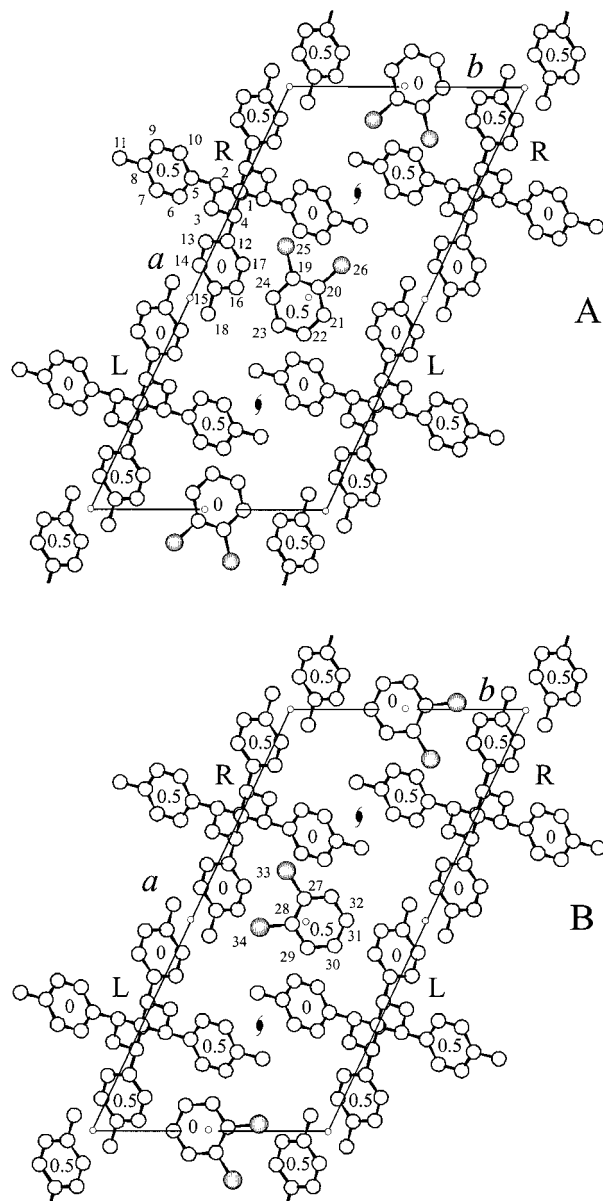
Figure 4. Two models of packing for the crystal structure of the clathrate form of s-PPMS containing *o*-DCB in the space group $P2_1/a$. The models present a different positioning of the *o*-DCB molecules. For each model (A and B), only one of the two possible centrosymmetric positions of the *o*-DCB molecule is shown. In the crystal structure a disorder in the position of the *o*-DCB molecules in the cavities characterized by the statistical arrangement of the *o*-DCB molecules in the two positions A and B, is present. The atoms of the asymmetric unit are labeled. The approximate z/c fractional coordinates of the barycenters of the phenyl rings are also shown. R = right- and L = left-handed chain.

with the inversion center at $x/a = 0.5$, $y/b = 0.5$, and $z/c = 0.5$, and then its position was varied during the minimization. Two nearly isoenergetic minima, corresponding to two slightly different positions of the guest molecules, were found through the minimization procedure. The models of packing corresponding to these energy minima are shown in parts A and B of Figure 4. A $cb \sin \gamma$ projection of the model of Figure 4B is also shown in Figure 5. It is worth noting that in these models the chlorine atoms occupy statistical positions of the benzene ring as required by the presence of the inversion center.
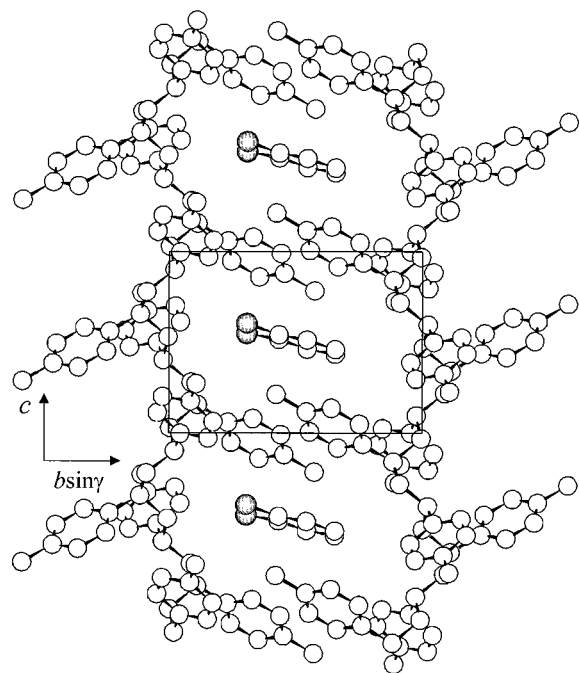
Figure 5. *cb* sin γ projection of the model of packing of Figure 4B. Only the chains of s-PPMS delimiting the cavities (with axes at *x/a* = 0.25, *y/b* = 0; and *x/a* = 0.75, *y/b* = 1) and the *o*-DCB molecules that are inside the cavities centered at *x/a* = 0.5 and *y/b* = 0.5, are shown.

Minimizations of the packing energy were also performed, starting from different orientations of the polymer chains, corresponding to different points inside the low-energy region of the map of Figure 3, but models of packing similar to those displayed in parts A and B of Figure 4 were obtained.

The feasibility of the different models of packing corresponding to the packing energy minima has been verified by calculations of structure factors. Both the models of parts A and B of Figure 4 give good agreement between the calculated structure factors and the intensities observed in the X-ray fiber diffraction pattern of Figure 1. The best agreement is however achieved for a statistical model characterized by *o*-DCB molecules arranged statistically in the positions corresponding to the models of parts A and B of Figure 4. These results suggest that a positional disorder of the guest molecule inside the cavity is probably present.

The intensities of the reflections in the X-ray diffraction pattern depend on changes in the *o*-DCB content of the analyzed sample. Structure factor calculations have been also performed by varying the occupancy factors of the atoms of *o*-DCB molecule. The best agreement is obtained when all the cavities are occupied by the *o*-DCB molecules.

The fractional coordinates of the carbon and chlorine atoms of the asymmetric unit, in the model of Figure 4, are listed in Table 2. The calculated structure factors are compared in Table 3 to the experimental structure factors evaluated from the X-ray fiber diffraction pattern of Figure 1. A fairly good agreement is apparent; the final discrepancy factor is *R* = 15.8%, for all observed reflections.

In the crystal structure right- and left-handed helical chains alternate along the *a* axis, and in this direction, there is no space for including the *o*-DCB molecules. On the contrary, between adjacent chains along the (*a*/2 + *b*) direction, one *o*-DCB molecule can be accommodated

Table 2. Fractional Coordinates of the Atoms of the Asymmetric Unit in the Models of Figure 4 for the Clathrate Form of s-PPMS with *o*-DCB, Where the Asymmetric Unit Corresponds to the Two Monomeric Units of the s-PPMS Chains and the Atoms of *o*-DCB Labeled in Parts A and B of Figure 4

	x/a	*y/b*	*z/c*	occupancy factor
C1	0.248	−0.004	0.530	1
C2	0.234	−0.113	0.657	1
C3	0.289	−0.088	0.780	1
C4	0.306	0.023	0.903	1
C5	0.218	−0.233	0.560	1
C6	0.262	−0.246	0.450	1
C7	0.247	−0.357	0.362	1
C8	0.188	−0.456	0.383	1
C9	0.144	−0.443	0.492	1
C10	0.159	−0.332	0.581	1
C11	0.172	−0.576	0.286	1
C12	0.366	0.045	0.999	1
C13	0.368	−0.045	0.113	1
C14	0.423	−0.025	0.201	1
C15	0.477	0.085	0.176	1
C16	0.475	0.175	0.063	1
C17	0.420	0.155	0.974	1
C18	0.537	0.107	0.272	1
C19	0.453	0.396	0.526	0.25
C20	0.473	0.521	0.465	0.25
C21	0.439	0.600	0.450	0.25
C22	0.584	0.554	0.495	0.25
C23	0.564	0.429	0.556	0.25
C24	0.498	0.351	0.571	0.25
Cl25	0.347	0.302	0.547	0.25
Cl26	0.422	0.577	0.411	0.25
C27	0.449	0.434	0.517	0.25
C28	0.509	0.435	0.542	0.25
C29	0.565	0.546	0.513	0.25
C30	0.561	0.657	0.460	0.25
C31	0.500	0.657	0.435	0.25
C32	0.444	0.546	0.463	0.25
Cl33	0.383	0.307	0.550	0.25
Cl34	0.516	0.307	0.604	0.25

in an isolated cavity delimited by phenyl rings of two enantiomorphic chains as shown in Figure 5. This cavity is also shown in Figure 6, where the effective space available for the *o*-DCB molecule is shown. All the contacts distance between the carbon atoms of the polymer chains are at least 3.9 Å, with the exception of one distance, between the carbon atoms of the phenyl rings of adjacent chains along *a*, that was found of 3.7 Å. Few contact distances between the carbon atoms of the *o*-DCB molecule and phenyl ring of the polymer chains are in the range 3.6−3.7 Å; all the other distances are greater than 3.8 Å.
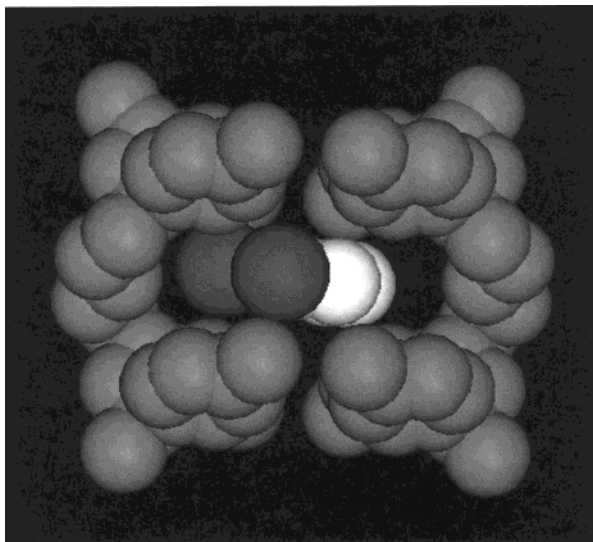
Concluding Remarks

The crystal structure of the clathrate form of s-PPMS containing *o*-DCB has been determined by the analysis of the X-ray fiber diffraction pattern and packing energy calculations.

The proposed model could be considered as representative of the crystal structure of α class clathrates of s-PPMS.[14] The crystal structure of the clathrates belonging to the α class, that is containing *o*-xylene, *o*-chlorophenol, and *N*-methyl-2-pyrrolidone as guest molecules are probably very similar to that of the clathrate with *o*-DCB.

Remarkable differences there exist between the crystal structure of the clathrate with *o*-DCB (α class) and that of the clathrate with THF, representative of the clathrates of the β class.[15] A common feature is the

Table 3. Comparison between the Calculated Structure Factors (F_c) for the Statistic Model of the Clathrate Form of s-PPMS with *o*-DCB of Figure 4 and the Observed Structure Factors (F_o), Evaluated from the Intensities Observed in the X-ray Fiber Diffraction Pattern of Figure 1[a]

h k l	d_{obs} (Å)	d_{cal} (Å)	F_c	F_o
0 1 0 2 0 0	10.65	10.72 10.60	50 35 {61}	67[b]
2 1̄ 0	9.60	9.92	138	160
2 1 0		6.32	59	
2 2̄ 0		5.89	31	
4 1̄ 0 0 2 0 4 0 0	5.47	5.83 5.36 5.30	61 120 81 {157}	191
4 2̄ 0	4.87	4.96	89	48
2 2 0		4.13	38	
4 1 0		4.11	45	
2 3̄ 0 6 1̄ 0 4 3̄ 0	3.87	3.93 3.88 3.80	25 39 25 {53}	38
6 2̄ 0		3.77	22	
0 3 0	3.63	3.57	70	63
6 0 0		3.53	20	
4 2 0 2 3 0 6 1 0	3.16	3.16 3.02 3.00	10 58 60 {84}	75
8 2̄ 0 2 4̄ 0	2.93	2.91 2.91	49 67 {83}	79
8 1̄ 0		2.87	41	
6 4̄ 0 8 3̄ 0 8 0 0	2.67	2.77 2.76 2.65	36 45 40 {70}	84
4 3 0		2.51	31	
6 2 0		2.50	38	
2 4 0		2.37	36	
4 5̄ 0		2.37	35	
8 1 0		2.35	30	
6 5̄ 0		2.32	29	
10 3̄ 0		2.30	30	
1 0 1	7.28	7.23	20	27
1 1̄ 1		6.44	47	
0 1 1 2 1̄ 1	6.12	6.25 6.08	19 31 {36}	40
1 1 1	5.69	5.63	240	271
3 1̄ 1 3 0 1	5.28	5.38 5.20	107 156 {189}	110
2 1 1		4.88	48	
2 2̄ 1		4.68	19	
4 1̄ 1		4.64	18	
1 2̄ 1		4.64	23	
3 2̄ 1 0 2 1 4 0 1	4.43	4.50 4.40 4.36	142 106 75 {193}	184
4 2̄ 1 1 2 1 5 1̄ 1	4.05	4.17 4.04 4.00	199 32 94 {222}	220
5 2̄ 1 5 0 1	3.83	3.77 3.71	50 56 {75}	100
2 2 1		3.64	17	
4 1 1		3.62	24	
3 3̄ 1 2 3̄ 1 6 1̄ 1 4 3̄ 1 1 3̄ 1 6 2̄ 1	3.35	3.50 3.50 3.46 3.41 3.40 3.39	86 24 12 63 60 79 {148}	156
3 2 1		3.26	41	
5 3̄ 1		3.24	37	
0 3 1		3.24	38	
6 0 1		3.21	19	
5 1 1		3.16	43	
6 3̄ 1 1 3 1 7 1̄ 1 7 2̄ 1 4 2 1	2.97	3.04 3.03 3.03 3.03 2.92	23 18 48 63 23 {87}	102
7 0 1		2.82	13	
2 3 1		2.81	25	
6 1 1		2.79	42	
3 4̄ 1		2.76	29	
4 4̄ 1		2.75	45	
8 2̄ 1		2.72	19	
2 4̄ 1		2.72	16	
8 1̄ 1		2.69	11	
1 4̄ 1		2.64	33	
5 2 1		2.63	31	
8 3̄ 1		2.60	29	
0 0 2		3.84	157	n.e.[c]
1 1̄ 2 0 1 2 2 1̄ 2	3.64	3.65 3.62 3.58	132 70 170 {226}	293
1 1 2		3.49	11	
3 1̄ 2 3 0 2	3.38	3.42 3.38	22 50 {55}	54
2 1 2		3.28	13	
4 1̄ 2 1 2̄ 2 3 2̄ 2 0 2 2 4 0 2	3.16	3.21 3.21 3.16 3.12 3.11	20 78 16 29 34 {93}	95
4 2̄ 2 1 2 2 5 1̄ 2 5 2̄ 2	2.99	3.04 2.99 2.97 2.88	55 16 87 75 {128}	116
5 0 2		2.85	12	
3 3̄ 2 2 3̄ 2 4 3̄ 2 1 3̄ 2 6 2̄ 2	2.71	2.75 2.75 2.70 2.70 2.69	88 82 11 14 32 {125}	83
5 3̄ 2		2.62	49	
0 3 2		2.62	19	
6 0 2		2.60	23	
1 3 2		2.50	13	
7 2̄ 2		2.50	61	
4 2 2		2.44	13	
7 0 2		2.38	17	
7 3̄ 2		2.38	19	
4 4̄ 2 8 2̄ 2 2 4̄ 2 5 4̄ 2 8 1̄ 2	2.32	2.34 2.32 2.32 2.31 2.30	42 30 64 20 15 {86}	89
6 4̄ 2		2.25	16	
8 3̄ 2		2.24	23	
3 3 2		2.24	16	
0 4 2 8 0 2	2.21	2.20 2.18	46 46 {65}	65
7 1 2		2.17	14	
7 4̄ 2		2.17	14	
9 2̄ 2		2.15	61	
9 1̄ 2 9 3̄ 2 4 3 2 6 2 2 8 4̄ 2	2.10	2.12 2.10 2.10 2.10 2.08	53 28 15 33 54 {82}	72
2 4 2 4 5̄ 2 9 0 2 8 1 2 3 5̄ 2 10 2̄ 2 2 5̄ 2 5 3 2	1.98	2.02 2.01 2.01 2.01 2.00 1.98 1.97 1.97	31 82 49 23 16 27 18 29 {113}	103

[a] The Bragg distances observed (d_{obs}) in the X-ray diffraction pattern and calculated (d_{cal}) for the unit cell with axes 23.4 Å, $b = 11.8$ Å, $c = 7.7$ Å, and $\gamma = 115°$ are also reported. Reflections with F_c less than 10 have not been reported. [b] The intensity of this reflection was evaluated by comparison with the intensity of the reflection 2 1̄ 0 from the X-ray powder diffraction pattern reported in Figure 5 of ref 2. [c] n.e. = not evaluated.

presence of **s**(2/1)2 helical chains packed in monoclinic unit cells, according to the space group $P2_1/a$. Relevant differences are concerned with the position of the guest molecules in the unit cell. In the crystal structure of the clathrate of s-PPMS with THF, the guest molecules occupy cavities around the 2-fold screw axes of symmetry, between phenyl rings of isomorphic adjacent polymer chains along the *b* axis of the unit cell.[15] The THF molecule is small enough to enter into the cavity formed by the four phenyl rings of a single s-PPMS chain (Figures 6 and 8 of ref 15). In this structure the cavities are not isolated and the guest molecules are connected through the 2-fold crystallographic symmetry. They could interact each other, since the distance between subsequent THF molecules, along the *c* axis, is 4.0 Å (see Figure 8 of ref 15).

Figure 6. View of the model of Figure 4B showing the van der Waals encumbrance of the carbon and chlorine atoms of and the effective space available for the accommodation of the *o*-DCB molecule. For clarity, the hydrogen atoms are not shown.

In the structure of the s-PPMS clathrate with *o*-DCB, the guest molecules are in isolated cavities located around a crystallographic inversion center and delimited by the phenyl rings of two enantiomorphic helical chains (Figure 6). This kind of cavities are very similar to the cavities present in the crystal structure of the clathrate forms of s-PS,[7−10] the guest molecules are isolated, the distances between two subsequent guest molecules, along the *c* axis, being nearly 8 Å.

On the basis of the present knowledge, we can conclude that s-PPMS form two kind of clathrate structures, depending on the steric hindrance of the guest molecules; small cyclic molecules with ring composed by five or six atoms (belonging to the β class) are able to enter into the cavity formed by the four phenyl rings of a single s-PPMS chain, giving rise to a kind of packing similar to the s-PPMS/THF clathrate. Bigger ortho-substituted molecules, belonging to the α class, can be accommodated only in bigger cavities formed by the phenyl rings of two adjacent enantiomorphic chains, as occurs in all the clathrates of s-PS.

References and Notes

(1) Iuliano, M.; Guerra, G.; Petraccone, V.; Corradini, P.; Pellecchia, C. *New Polym. Mater.* **1992**, *3,* 133.
(2) De Rosa, C.; Petraccone, V.; Guerra, G.; Manfredi, C. *Polymer* **1996**, *37*, 5247.
(3) Guerra, G.; Iuliano, M.; Grassi, A.; Rice, D. M.; Karasz, F. E.; McKnight, J. *Polym. Comm.* **1991**, *32*, 430.
(4) Guerra, G.; Dal Poggetto, F.; Iuliano, M.; Manfredi, C. *Makromol. Chem.* **1992**, *193*, 2413.
(5) Immirzi, A.; De Candia, F.; Iannelli, P.; Vittoria, V.; Zambelli, A. *Makromol. Chem., Rapid Commun.* **1988**, *9*, 761.
(6) Guerra, G.; Vitagliano, V. M.; De Rosa, C.; Petraccone, V.; Corradini, P. *Macromolecules* **1990**, *23*, 1539.
(7) Chatani, Y.; Inagaki, T.; Scimane, Y.; Shikuma, H. *Polymer* **1993**, *34*, 1620.
(8) Chatani, Y.; Scimane, Y.; Inagaki, T.; Ishioka, T.; Ijitsu, T.; Yukinari, T.; Shikuma, H. *Polymer* **1993**, *34*, 4841.
(9) De Rosa, C.; Guerra, G.; Petraccone, V.; Pirozzi, B. *Macromolecules* **1997**, *30*, 4147.
(10) De Rosa, C.; Rizzo, P.; Ruiz de Ballestreros, O.; Petraccone, V.; Guerra, G. *Polymer* **1999**, *40,* 2103.
(11) Guerra, G.; Manfredi, C.; Musto, P.; Tavone, S. *Macromolecules* **1998**, 31, 1329.
(12) Guerra, G.; Milano, G.; Venditto, V.; Loffredo, F.; Ruiz De Ballesteros, O.; Cavallo, L.; De Rosa, C. *Macromol. Symp.* **1999**, *138*, 131.
(13) Guerra, G.; Milano, G.; Venditto, V.; Musto, P.; Cavallo, L.; De Rosa, C. *Chem. Mater.* **2000**, *12*, 363.
(14) Dell'Isola, A.; Floridi, G.; Rizzo, P.; Ruiz de Ballestreros, O.; Petraccone, V. *Macromol. Symp.* **1997**, *114*, 243.
(15) Petraccone, V.; La Camera, D.; Pirozzi, B.; Rizzo, P.; De Rosa, C. *Macromolecules* **1998**, *31*, 5930.
(16) Rizzo, P.; Ruiz De Ballesteros, O.; Auriemma, F.; De Rosa, C.; La Camera, D.; Petraccone, V.; Lotz, B. *Polymer* **2000**, *41*, 3745.
(17) Cromer, D. T; Mann, J. B. *Acta Crystallogr.* **1968**, *A24*, 321.
(18) Kong, Y.; Ponder, J. W. *J. Chem. Phys.* **1997**, *107*, 481.
(19) Yoon, D. Y.; Sundararajan, P. R.; Flory, P. J. *Macromolecules* **1975**, *8*, 776.
(20) Sundararajan, P. R.; Flory, P. J. *J. Am. Chem. Soc.* **1974**, *96*, 5025.
(21) Suter, U.; Flory, P. J. *Macromolecules* **1975**, *8*, 765.
(22) Brant, D.; Miller, W.; Flory, P. J. *J. Mol. Biol.* **1967**, *23*, 47.
(23) Ketelaar, J. *Chemical constitution*; Elsevier: New York, 1958.
(24) Hopfinger, A. *Conformational properties of macromolecules*; Academic Press: New York, 1979.

MA991936Z